ON AC CIRCUITS AND ELECTROMAGNETISM

A. BAKSHI
Data Analyst, Experiment Design

M. CHEN
Experiment Design, Notebook Manager

J. HUANG
Data Analyst, Notebook Manager

J. LIN
Data Analyst, Editor, Experiment Design

J. LIU
Data Analyst, Experiment Design

(Received on December 19, 2017)

This paper details the capabilities of common circuits as measured by a variety of experiments, including analysis of impedance in relation to inductance and capacitance. These experimental capabilities were generally consistent with theory. A V-i phase shift of $(37.02 \pm .02)^\circ$ was predicted in the RC circuit, and a $(36.7 \pm .1)^\circ$ phase shift was observed. This resulted in a expected Lissajous figure. In the CLR circuit, a resonance frequency of (15890 ± 20)Hz was observed, and a current damping curve $i(t) = (-2.83 \pm .02\text{E}{-4})e^{-2500 \pm 50t} sin((-2.83 \pm .02\text{E}{-4})t)$ was modelled. The CLR results were then applied to a transformer which behaved like a parallel CLR circuit at high frequencies. Magnetic principles such as the Biot-Savart Law were also applied to design and thoroughly test a Matlab simulation. Several results followed the comparison of experimental and theoretical values with solenoids, for example, the elapsed lifespan of the Hall-Effect probes was estimated to be 0.8 years.

I INTRODUCTION

Alternating current (AC) and electromagnetism are the basis for all modern electronics; their inventions paving the way for efficient designs in phones, computers, and radios. Using equipment, and basic circuit analysis, common components of circuits (such as capacitors and inductors) can be tested. Furthermore, magnetic fields generated by solenoids were also investigated.

II THEORY

Several accepted principles and theories were used in our circuit analysis. The wires in the circuits are assumed to be ideal conductors. As such, Ohm's law is used to find the current, voltage, or resistance across an ideal conductor. The general form is:

$$V = iZ \qquad [1]$$

(*HRW 2017*)

Where:
V = The potential through the load (V)
i = The current through the load (A)
Z = The impedance (Ω)

To calculate total impedance and phase shift when a reactive component is in a circuit, the following two equations can be used.

$$Z = \sqrt{R^2 + {X_T}^2} \qquad [2]$$

(*HRW 2017*)

$$\phi = \arctan\left(\frac{X_T}{R}\right) \qquad [3]$$

(*HRW 2017*)

Where:
Φ = The phase angle (rad)

Z = The total impedance(Ω)
R = The total resistance (Ω)
X_T = The total reactance (Ω)

Furthermore, the reactance of inductors and capacitors in an AC circuit can be calculated using the following.

$$X_L = \omega L \qquad [4]$$
(*HRW 2017*)

$$X_C = \frac{1}{\omega C} \qquad [5]$$
(*HRW 2017*)

Where:
X_L = Reactance of the inductor (Ω)
X_C = Reactance of the capacitor (Ω)
ω = Angular frequency (rads^{-1})

The frequency at which total reactance is zero is presented by the following.

$$f_r = \frac{1}{2\pi\sqrt{LC}} \qquad [6]$$
(*HRW 2017*)

Where:
X_L = Reactance of the inductor (Ω)
X_C = Reactance of the capacitor (Ω)
ω = Angular frequency (rads^{-1})

III Method

The internal impedance of the function generator was in series with the power supply. Additional resistances were added to the configuration and the potential across the function generator were measured. The internal resistance of the function generator was calculated by comparing the potential ratios.

A $(46.2 \pm .3)$ Ω resistor and $(98.2 \pm .1)$ μF capacitor were connected in series to an AC function generator to create an RC circuit. The frequency was set to $(47.0 \pm .5)$ Hz to obtain a reasonable phase shift. The potential was measured with a LabQuest across the resistor and across both the resistor and the capacitor.

A CLR circuit was constructed with a $(51.0 \pm .2)$ Ω resistor, $(9.8 \pm .2)$ mH inductor and $(10.2 \pm .1)$ nF capacitor. An LC circuit was in a configuration such that a switch would disconnect the capacitor from a potential source and connect it to an inductor. Then, the natural frequency of this circuit was measured with an oscilloscope. By introducing a switch in the circuit, a closed loop containing just CLR can be constructed. When the switch is closed, the current continues to oscillate in the loop as it is slowly damped by the resistor.

Two solenoids, one of 300 coils and the other of 1200, and iron magnetic cores were used to create a transformer with a 4:1 step-up ratio. A function generator was connected to the primary winding. The input and output potentials were then measured.

For the B-field experiments, a retort stand and clamp were used to secure the probe to minimize fluctuations in the Hall effect sensor readings. Using the LabQuest, an average was produced and recorded over 10 seconds at 25 measurements per second. In the final experiment, multiple configurations were verified by the simulation, which was then replicated in the laboratory. The method used in experiment 4 was repeated with some additions. Retort stands were used to ensure that the coils remained in its desired angles. Tape measures and grid paper were secured on the lab bench to create a coordinate system that gave the position of the probe.

IV Analysis

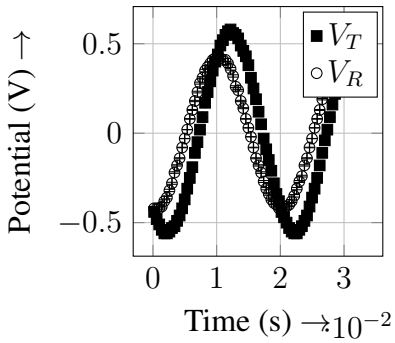

Fig. 1. Potential vs. time functions of V_R and V_T. with their respective sinusoidal fit. The phase shift between i_T and V_T is clearly visible on the graph.

The RC phase shifts created with components used in the previous DC lab are only reasonable at very low frequencies (<1Hz). Therefore, different components were used to obtain an RC phase shift and conform to impedance matching.

The reactance of the capacitor can be obtained using [2], with the total impedance defined as the ratio between max potential and current. A capacitive reactance of $(33.6 \pm .2)\Omega$ was found compared to the theoretical $(34.5 \pm .2)\Omega$.

In an AC series circuit, the current is in phase with $V_{Resistor}$ and lags 90° behind $V_{Capacitor}$. Combining these components produced a phase angle between 0° and 90°. Since the current is in phase with the potential across the resistor, the V_R-t graph had the same phase shift as the i_T-t graph with respect to the V_T-t graph. The Solver tool in Excel generated a sinusoidal fit of

$$V_R = 0.428 \pm .002(sin((314.2.3)t + 1.63 \pm .04) \quad [7]$$

$$V_T = 0.560 \pm .003(sin((314.2.3)t + 2.28 \pm .05) \quad [8]$$

From this, a phase angle of $(37.02 \pm .02)°$ was computed as the difference in the phase shifts of the two sinusoidal fits. The theoretical phase angle between potential and current is $(36.7 \pm .1)°$ as computed by [3].

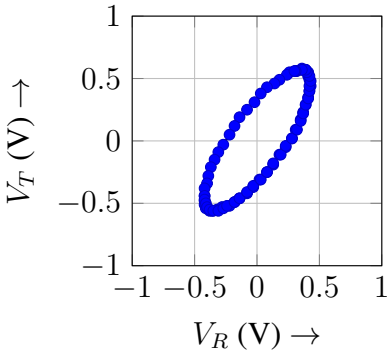

Fig. 2. The Lissajous figure alongside its theoretical fit. The line represents its fit, while individual data points are shown.

The Lissajous figure was generated by plotting V_T vs V_R, which was modeled by a parametric equation. The Lissajous figure appears to be continuous, which implies that V_R and V_T had a very similar frequency as expected.

An interesting characteristic of an RC circuit became apparent in the frequency domain. Using [5], as the frequency approaches 0, the reactance goes to infinity, whereas when the frequency approaches infinity, the reactance goes to zero. It can be determined that V_C is approximately V_S at low frequencies and V_R is approximately V_S at high frequencies. This effect has practical applications and can be used to create high-pass and low-pass filters.

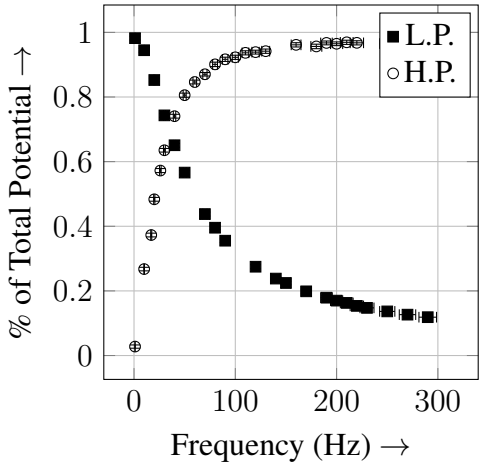

Fig. 3. Plot for a Low and High Pass filter. The Low Pass is represented by the potential across the capacitor and High Pass is the potential across the resistor. A low-pass filter would take potential across capacitor and a high-pass would take potential across the resistor. The intersection point, which was graphically determined to be $(35.1 \pm .4)$Hz is one bound for both filters.

The reactance vs. frequency of the inductor is proportional to the frequency while that of a capacitor is inversely proportional. Additionally, the current in an inductor leads the potential difference across it by 90°, therefore its phasor is exactly opposite to its capacitor counterpart. When the magnitudes of capacitive reactance and inductive reactance are equal, they cancel each other out.

The frequency this occurs at is described by [6], and is called the resonance frequency.

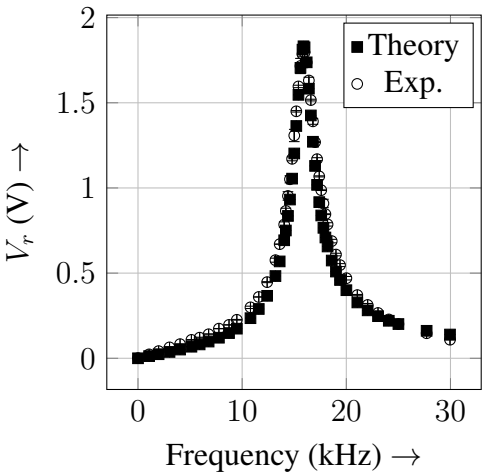

Fig. 4. V_r **vs frequency of the RLC circuit.** The peak of the plot represents the resonance frequency where the reactive component of the impedance is zero

A GRG nonlinear regression was performed and a peak frequency was determined to occur at (15893 ± 1)Hz, which is close to the predicted value of (15919 ± 7)Hz using [6].

The resonance frequency of the described circuit is dependent on the driving source. However, if the driving source is removed, the oscillation will continue, decaying at a rate based on the resistance of the circuit.

The damping response of the RLC circuit was due to the resistor exhibiting Joule heating, the process of converting electrical current into heat. To model this, the Laplace transform was applied to a differential equation obtained from Kirschoffs Circuital Laws, putting it in the s-domain. A solution was then algebraically determined, and after an inverse Laplace transformation, the solution in the t-domain was obtained as follows.

$$i(t) = (-2.83 \pm .02\text{E}{-4})e^{-2500 \pm 50t} \\ sin((-2.83 \pm .02\text{E}{-4})t) \quad [9]$$

[9] defines an underdamped transient response. Unfortunately, the time constant was very small, resulting in the oscillations dying out faster than can reliably be measured. The results of this experiment were inconclusive.

The frequency at which the LC circuit oscillated at was (15906 ± 5)Hz, confirming the theoretical mechanisms of a capacitor and inductor.

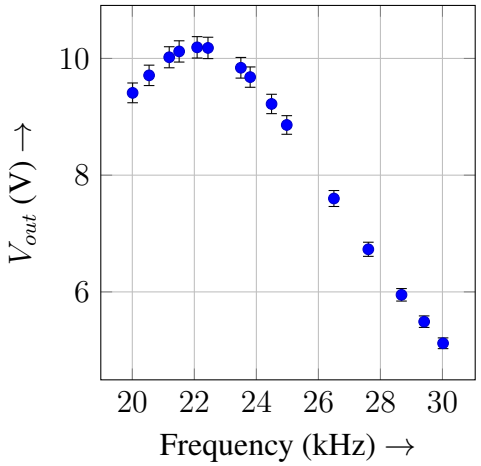

Fig. 5. V_{out} **vs frequency plot of the transformer.** A peak potential can be observed at $(22.3 \pm .2)$kHz.

The output potential difference began to drop off at $(22.3 \pm .2)$kHz. The energy losses in a transformer were primarily due to winding and core losses. Some losses were unavoidable and not connected to frequency such as Joule heating through the windings. However, effects such as hysteresis loss and Eddy current losses exist within the core and are directly related to frequency. The energy losses in the transformer can be attributed to these factors.

Another possible explanation for the behaviour of the transformer is a result of all solenoids possessing a parasitic capacitance, which becomes more apparent as the frequency increases. This results in the solenoid behaving like a capacitor. This parasitic capacitance effectively renders the transformer into a parallel RLC circuit, with the resistance of the circuit originating from the resistance of the wire, with its resonance near the peak of figure 5.

Many mathematical models were explored but none were sufficient due to the complexities of the transformer.

The experimental square solenoid data aligned within a margin of error of the simulation, most likley due to a change in ambient per point.

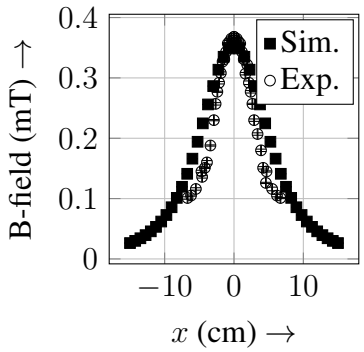

Fig. 6. Graph of a 300 coil square solenoid. Experimental data lie extremely close to the theoretical values.

Parallel Helmholtz coils proved to be more interesting. Setting the distance in between to the radius of the two coils, minimizes the variation of the magnetic field strength in between, whereas setting a distance greater to the radius creates a bimodal sequence of points as seen in figure 7.

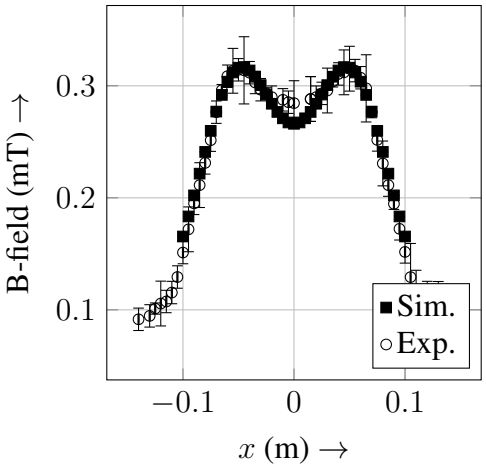

Fig. 7. Graph of the magnetic field of coils at 10.5cm apart. The experimental and simulated values differed little, likely due to the change in ambient between points. A common dip occurs at x=0

Because the other coil isnt there to reinforce the magnitude of the B-field, there is a slight drop before the peak of the second coil is obtained. This reinforced the idea that B-fields add linearly, and experiment 5 was designed to verify this claim.

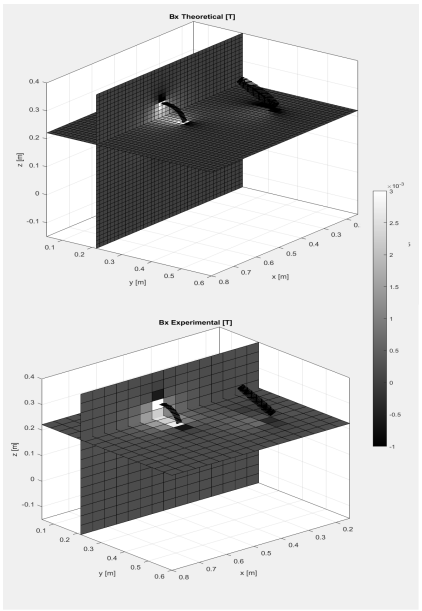

Fig. 8. Simulation of the magnitude of the orientation. The top plot is the simulated values and the bottom plot is the experimental value. Notice the change in magnitude is minimal, but higher magnitudes are noted in the experiment.

It can be noted that, at the x=47.6cm plate, the experiment 5 plot (figure 8) greatly deviates from the expected values. The fact that this specific probe caused erroneous readings gave reason for suspicion. Studies performed by Liu et al. (1998) reveal that most hall effect probes are aligned in a cross-shaped sensor. The potential across two of the plates are used to compute the magnetic field. However, once this potential is altered, the reading changes as well.

According to Paun et al. (2003), the correction factor would be as shown.

$$G = 1 - 5.0267\frac{\theta_H}{\tan(\theta_H)}\exp\left(\frac{\pi L}{2W}\right) \quad [10]$$

(*Paun 2013*)

Where:
G = The geometric correction factor
θ_H = The Hall angle

Consistent usage will often break down one end of the plate. Such change will inevitably alter the symmetry of the hall effect probe itself, causing a shift in the Hall Angle. From the experimental data, 0.8 years of usage was inferred. The equipment was found to have been in use for 5-6 years. As such, consistent usage rate (between labs and the Algonquin Expedition) would add to around 0.8 years, verifying the error within the data.

What is interesting to note, however, is the presence of a magnetic field of magnitude $(-0.08 \pm .01)$ mT at areas where neither coil was facing, as in figure 9.

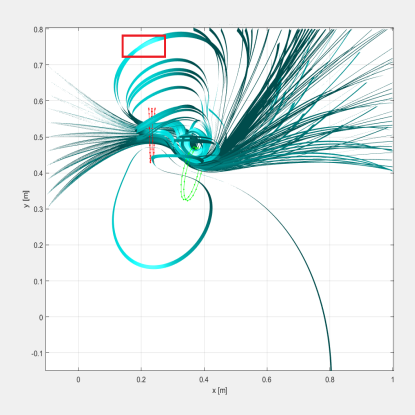

Fig. 9. Simulation of the magnetic field lines of the orientation. The red box represents the area with unexpected B-fields.

Using the simulation once again, the magnetic field lines were visualized at the spot of the magnetic field. Surprisingly, there exist chaotic field lines at that spot. As such, the basis of vector addition still holds.

To continue this investigation, a third, smaller, solenoid was energised and placed at a precomputed location. This was motivated by a desire to create a small volume with a net upwards magnetic field in the z direction. The results would be stunning, amidst all the chaos in the magnetic field, a small volume would be calm enough, in fact, that a small charged particle would be able to orbit around the field lines and parallel to the ground.

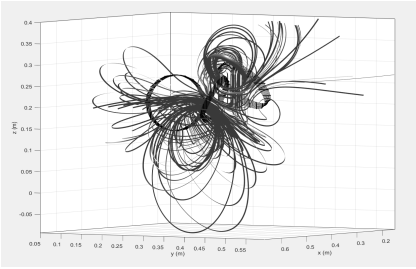

Fig. 10. Three solenoids and their respective flux tubes. Notice the deliberate phenomena set up in the upper right corner, the field lines are near vertical meaning the horizontal components of the B-field are negligible. The field lines are almost laminar amidst the remaining turbulence.

Unfortunately, for any charged particle of reasonable mass, the current needed was too large and could not be supplied.

V Sources of Error

The resistance and any inductive effects of the wires was not measured and assumed to be zero. Furthermore, different equipment was used across different days, leading to minor inconsistencies in the data.

Error could have been avoided when setting up the solenoids for circuits 4 and 5. This is due to the unmatchable precision required by theory. As demonstrated, even the smallest perturbation in position can cause drastic changes in B-field. Furthermore, the ambient b-field in the room was not well documented.

VI Conclusion

This report covers the simple yet ubiquitous phenomena in AC circuits and electromagnetism. Further research may be developed into exact cause and theoretical behavior of transformers at high frequencies, and magnetic field simulations where Biot-Savart law does not apply.

VII Sources

van Bemmel, Henri M., "1718 Lab Manual" 2017.

Halliday, D., Resnick, R. & Walker, "Fundamental of Physics." 2001.

Hirsch, Alan J. "Nelson Physics 11." 2002.

Kuphaldt, Tony R. "Lesson in Electric Circuits: an Encyclopedic Text & Reference Guide." 2011.

Liu, S., Guillou, H. & Kent, A. "Effect of Probe Geometry" 1998.

Makarov, Sergej N. Practical Electrical Engineering. 2016.

Paun, M., Sallese, J. & Kayal M. "Hall Effect Sensors." 2003.